Journal of Applied Polymer Science

UV grafting process for synthetic drag reduction of biomimetic riblet surfaces

Huawei Chen, Da Che, Xin Zhang, Deyuan Zhang
School of Mechanical Engineering and Automation, Beihang University, No. 37 Xueyuan Road, Haidian District, Beijing, 100191, China
Correspondence to: H. Chen (E-mail: chenhw75@buaa.edu.cn)

ABSTRACT: Skin–friction drag accounts for a large portion of resistance encountered by water-based vehicles, such as ships and submarines. Developing drag reduction methods to improve drag reduction performance has drawn worldwide attention recently. UV-induced polymerization has been investigated as a way to graft the drag reduction agent PAM on to a PVC substrate with a biomimetic riblet surface. The effects of AM concentration and irradiation time on the grafting rate were explored to determine optimal grafting parameters. UV grafting polymerization was clarified by comparing the peak absorption variation of the infrared spectrum before and after grafting. The PAM thin film grafted on riblet surface was measured approximately 10 μm in thickness. A rotating disk apparatus was built to measure the synthetic drag reduction performance. The drag reduction rate of the grafted PAM riblet surface was tested at approximately 14%, higher than the 6% of the traditional riblet surface. Moreover, the excellent drag reduction performance of grafted PDMS riblet surface lasted for 12 days. © 2015 Wiley Periodicals, Inc. J. Appl. Polym. Sci. **2015**, *132*, 42303.

KEYWORDS: application; biomimetic; photopolymerization

Received 17 December 2014; accepted 3 April 2015
DOI: 10.1002/app.42303

INTRODUCTION

Skin–friction drag accounts for a substantial portion of resistance in nearly all water-based vehicles, such as submarines.[1] Skin–drag reduction technology has attracted worldwide attention recently because it may have the potential to reduce fuel consumption. As the prospective drag reduction methods, a microgroove riblet surface and the addition of various drag reduction agents are still widely applied in various fields.

Over the past several decades, the shark skin has caught worldwide attention because of its superior drag reduction performance.[2,3] It has been demonstrated that drag reduction of shark skin is mainly created from the micro riblets formed by a perfect alignment of tiny scales over its entire body.[4] Walsh[5] investigated several different types of riblet surfaces and discovered that approximately 8% of the drag reduction occurred on a symmetric V-groove riblet. Bechert *et al.*[6] built an adjustable surface with longitudinal blade ribs and slits, based on systematic experimental optimization, and a maximum benefit of a 9.9% decrease in fluid drag was validated. Zhang *et al.* used shark skin as a direct replica to fabricate vivid shark skin surface and achieved drag reduction of approximately 8.25%.[7] Most of these biomimetic drag reduction studies take their inspiration from shark skin, in which a longitudinal V/U-groove riblet is set parallel to the direction of the flow of water. The main drawback of the biomimetic drag reduction riblet surface is that the maximum drag reduction is low (<10%).

To improve drag reduction performance, a drag reduction agent was intensively investigated recently as an alternative of drag reduction riblet, taking fish epidermal mucus as inspiration. Fringes *et al.*[8] conducted an experimental study of the impact of injecting concentrated polymer solutions into the near-wall region of a turbulent pipe flow and achieved 80% maximum drag reduction. Mizunuma *et al.*[9–12] tested the synergistic effects of turbulent drag reduction by pouring a great quantity of polymer additive directly into fluid. Christodoulou *et al.* carried out experiments on a combination of riblets and polymers to clarify the effect of Polyox 301 concentrations on drag reduction.[11] Drag reduction coatings have also been widely explored for their possible applications in outer fluid fields as substitutes for injection. Choi *et al.* found that the drag reduction of polymer-coated U-groove riblets was better than U-grooves alone in the experiment conducted in a rowing tank on a onethird scale model of the America's Cup winning yacht, the Australia II.[13] Zhang *et al.*[14] developed a synthetic drag reduction shark skin by grafting a long-chain drag reduction agent on to a water-born epoxy resin, and achieved a drag reduction of approximately 24.6%. However, the surface quality became unfavorable after 3 h of immergence in water. A great number of applications of drag reduction agents

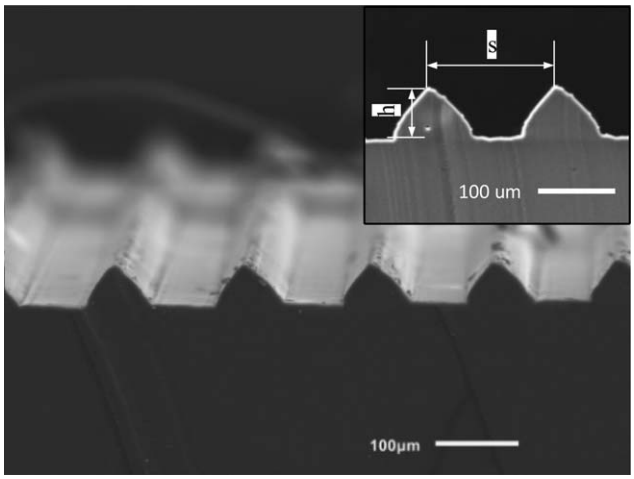

Figure 1. V-shape microgroove drag reduction riblet.

have demonstrated drawbacks, such as (1) waste of the polymer additive by injecting it into whole fluid, and (2) limited drag reduction improvement depending on the coating chosen.

With the problems of energy and environment becoming severe, a method of synthetic drag reduction that can simultaneously achieve higher drag reduction while using less polymer additive is becoming more necessary than ever. One novel UV-induced surface-grafting method has been developed to overcome drawbacks, such as low drag reduction and high cost. Synthetic drag reduction surfaces that are built by grafting PAM on to microgroove riblets have the following advantages: (1) the chemical reaction only takes place on the surface of substrate, so the bulk properties are not affected,[15] (2) high grafting efficiency,[15] (3) low cost,[15] and (4) suitability for large-area applications.[16] Apart from the UV-grafting process, synthetic drag reduction efficiency is validated by tests conducted in a rotating disk apparatus.

EXPERIMENTAL

Materials

The UV-induced grafting method is based on the traditional one-step grafting approach proposed by Yang and Rånby.[17–19] Various grafting experiments have been carried out for various materials, for example, PP,[20] PET,[20] Nylon,[20] and PAN.[20] In this paper, PVC is taken as a substrate to investigate the mechanism of UV grafting and synthetic drag reduction.

The substrates used in this experiment are soft polyvinyl chloride (PVC) film with a thickness of 0.5 mm. A 0.08-mm-thick polyester (PET) film with almost 100% UV transmittance (wavelength 200–400 nm) is used as a protective film to not only exclude oxygen but to also ensure that the solution—a mixture of monomer and acetone solvent—spreads flat. Benzophenone (BP, Tianjin Guangfu Fine Chemical Research Institute) is purchased and used as the photoinitiator. Acetone (Beijing Chemical Industry Group Company) is used as the solvent. Polyacrylamide (PAM, molecular weight >1,000,000, Tianjin Guangfu Fine Chemical Research Institute) is used as the drag reduction agent.[21] Acrylamide (AM, Molecular Weight 71.08, Tianjin Guangfu Fine Chemical Research Institute), the monomer of polyacrylamide (PAM), is applied for polymerization. A 1000 W high-pressure mercury lamp (Beijing Zhongruida Electric Light Factory) is chosen as the UV lamp.

Preparation of Synthetic Drag Reduction Surface

The processes of synthetic drag reduction preparation mainly consist of the fabrication of the biomimetic drag reduction riblet and the UV-induced grafting of PAM long-chains onto its surface.

Fabrication of Drag Reduction Riblet

A V-shape microgroove is used as the drag reduction riblet. The microgroove is rolled by use of a micro-grooved aluminum roller. The V-shape microgroove of the aluminum roller is machined using ultraprecision diamond cutting. The spacing (s) and height (h) of the machined riblet are approximately 150 and 60 μm, respectively, as shown in Figure 1.

UV-Induced Grafting of PAM Long Chains

The photografting polymerization system is shown in Figure 2, where a thin layer of the mixture is applied between the PET protection film and the PVC substrate. The protection film is pressed with suitable pressure to spread the mixture into an even and thin liquid layer. The extra solution is squeezed out and wiped off with a dry tissue paper. The UV lamp is fixed to the top of the substrate at a distance of approximately 50 cm.

All grafting polymerization is conducted inside a shaded ventilation cabinet. The temperature in this cabinet is controlled at 24°C. The reaction of photo-polymerization consists of two steps: first, the photografting of the monomer solutions to make the dormant end-groups covalently attach to the surface of the substrate, i.e., the photoinitiator BP introduces grafted chains on to the substrate. Second, UV irradiation induces the formation of surface free radicals and the re-activation of the dormant end-groups continuously. The mechanism of the photografting polymerization of the drag reduction agent is shown in Figure 3. After the grafting, the drag reduction surfaces are dipped into deionized water and then cleaned in ultrasonic cleaner for 20 min. Finally, the drag reduction surfaces are air-dried for 1–2 h. The grafting rate GR is defined to express the amount of AM grafted on to the PVC substrates by comparing the weights of the thin film before and after grafting, as expressed by:

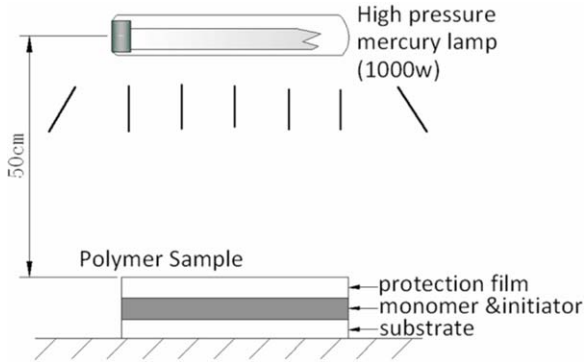

Figure 2. Schematics of photografting polymerization. [Color figure can be viewed in the online issue, which is available at wileyonlinelibrary.com.]

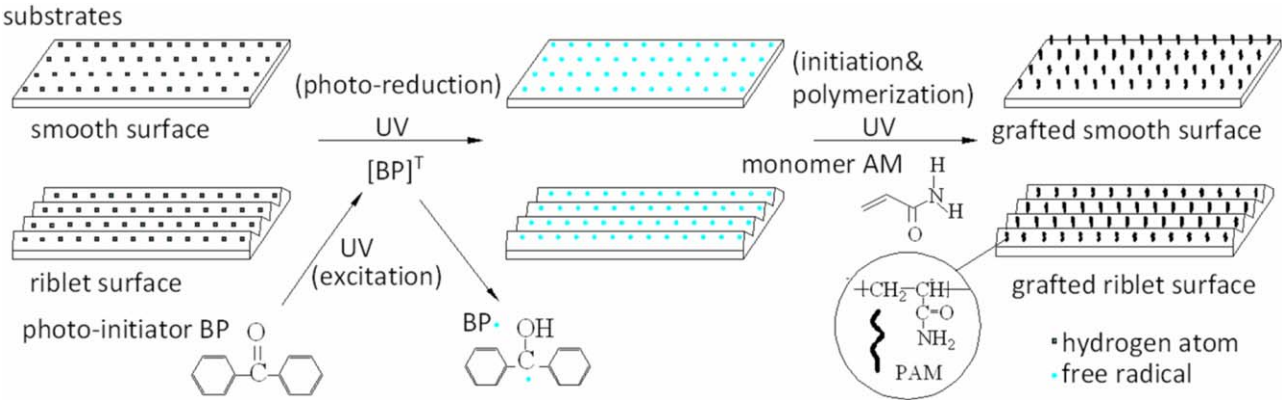

Figure 3. The reaction course of photografting initiated by BP. [Color figure can be viewed in the online issue, which is available at wileyonlinelibrary.com.]

$$GR = \frac{W_g - W_0}{W_0} \quad (1)$$

where W_0 is the weight of the substrates before grafting, and W_g is the weight of the substrates after grafting.

RESULTS AND DISCUSSION

Mechanism of Photo-Grafting Polymerization

In order to make clear the grafting mechanism, a micro-FTIR (Thermo Scientific Nicolet iN10MX) is used to determine the infrared spectrum of the PVC film before and after the grafting process. Using the spectrum, the functional groups and structures of the compounds can be identified from the functional group regions and fingerprint regions, respectively. Figure 4 shows the infrared spectrum of the PVC film before and after the grafting process. The absorption peaks near 1666 and 3397 cm^{-1} appear after the grafting, which represent the character of the carbonyl and hydroxyl groups, respectively. The appearance of carbonyl groups and hydroxyl groups on the surfaces indicates that the drag reduction agent PAM was formed on the surface of the substrates by grafting.

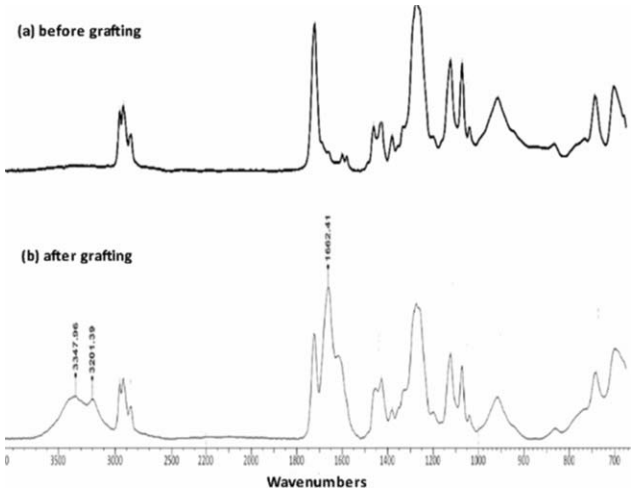

Figure 4. The infrared spectrum of the substrate before and after grafting. (1) The sharp absorption peak near 1666 cm^{-1}; i.e., the character of one of the carbonyl groups as it appears after grafting. (2) The obtuse round absorption peak near 3397 cm^{-1} indicates the character of one of the hydroxy groups.

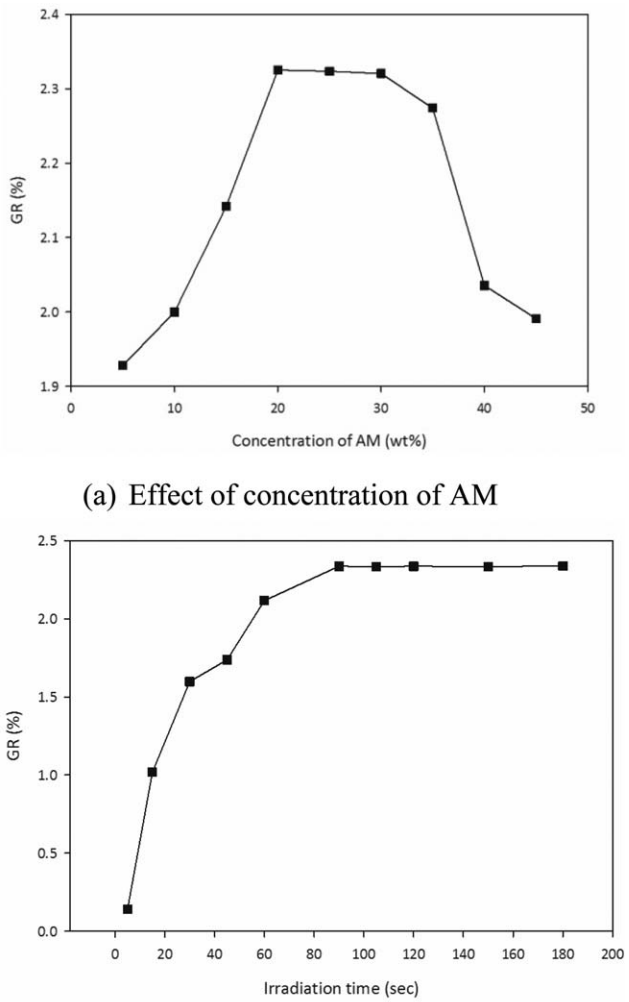

Figure 5. The changes of *GR* with the concentration of AM (a) and irradiation time (b).

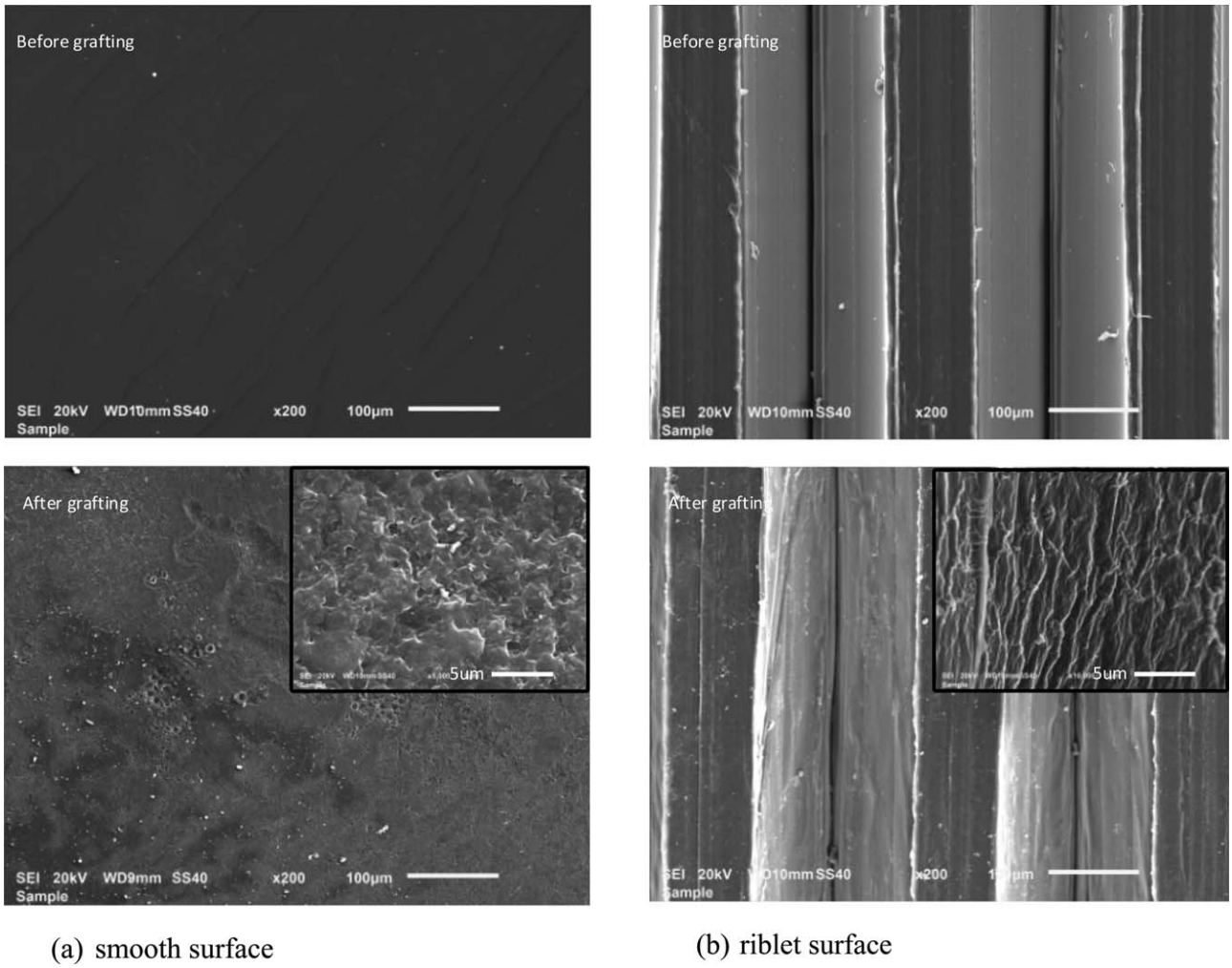

Figure 6. SEM images of smooth (a) and riblet (b) surfaces before and after grafting.

The concentration of BP in the photopolymerization experiments is chosen to be 5 wt %, referring to Yang and Rånby.[19] The variation of the grafting rate with the changes in the concentration of AM and the time of irradiation are measured as shown in Figure 5 to determine the concentration of AM and the various time of irradiation used in grafting. The irradiation time is set as 150 s to clarify the effect of the concentration of BP, and the concentration of AM is set at 20 wt % to investigate the effect of the irradiation time. As shown in Figure 5(a), the grafting rate initially rises with the increase of the concentration of AM, and then reaches a peak at approximately 2.35% as the concentration of AM approaches 20 wt %. The grafting rate gradually declines when the concentration of AM surpasses 30 wt %. The irradiation time also has a great impact on the grafting rate. The grafting rate improves with the increase in the irradiation time and is kept constant after approximately 100 s of UV irradiation, as shown in Figure 5(b), which implies that the entire reaction has been completed.

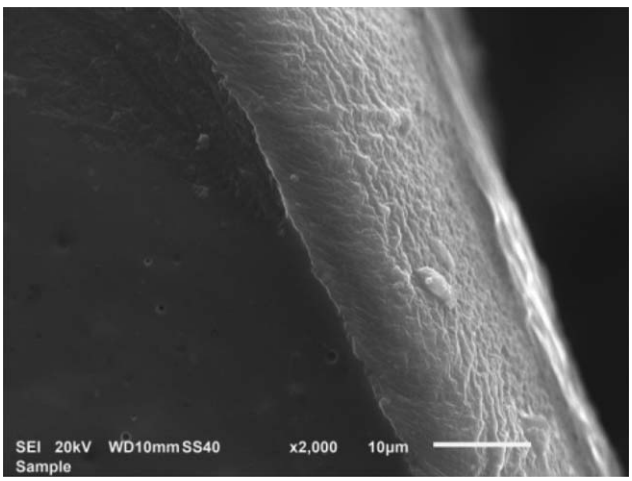

Figure 7. Thickness of grafted PAM thin film.

Drag Reduction Test of Synthetic Drag Reduction

Four kinds of test surfaces including smooth surface, PAM-grafted smooth surface, riblet surface, and PAM-grafted riblet surface were prepared to test their drag reduction. On the basis of the above-mentioned investigation of photoinduced grafting, a UV-induced grafting process was conducted at BP 5 wt %, AM 20 wt %, and an irradiation time of 150 s.

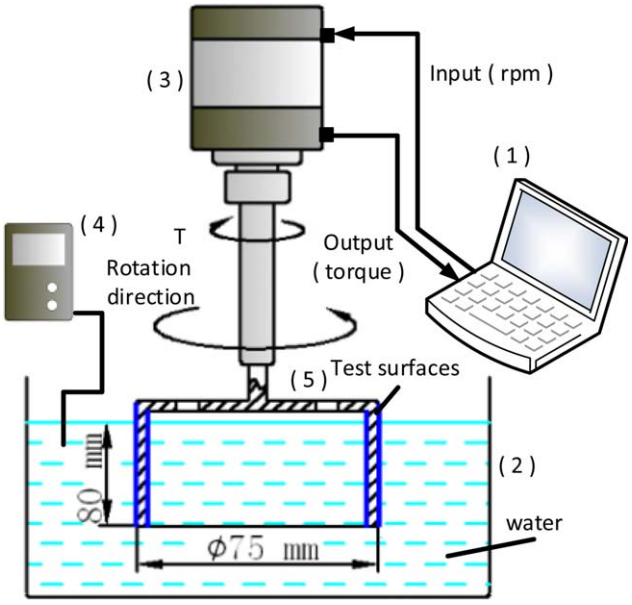

Figure 8. Experimental set-up of a rotating disk apparatus for drag reduction measurement: (1) PC, (2) water bath, (3) rotatory viscometer (Brookfield DV-III), (4) thermometer (TE1307), (5) test-rotor. [Color figure can be viewed in the online issue, which is available at wileyonlinelibrary.com.]

By comparing the surface quality of the thin film before and after grafting, as shown in Figure 6, we can see that the surface becomes rougher after grafting ($R_a < 0.6$), whether it was a smooth or a riblet surface. We also see that the shape of the drag reduction on the riblet remains almost unchanged, which indicates that the effect of the grafted surface roughness on surface drag can be ignored. The thickness of the grafted PAM thin film is measured at about 10 μm from the cross-section SEM photo, as shown in Figure 7.

A drag reduction testing platform is built to test the drag reduction of the synthetic drag reduction surfaces. The schematic diagram of the testing platform consists of a hollow cup-shaped aluminum barrel (the test rotor) with a diameter of 75 mm, a wall thickness of 3 mm and a height of 90 mm as shown in

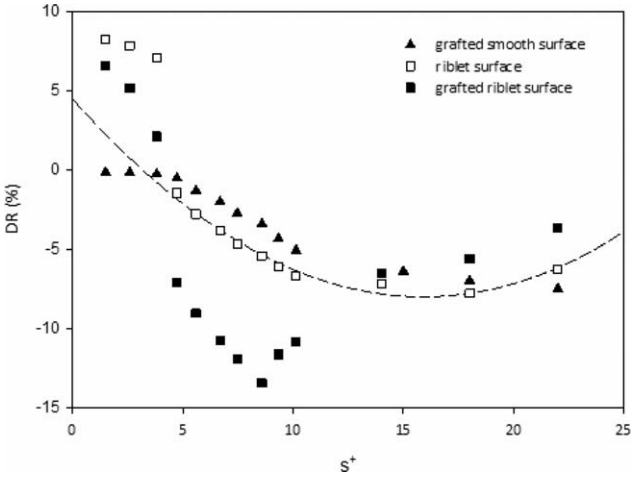

Figure 9. Drag reduction of three types of surfaces.

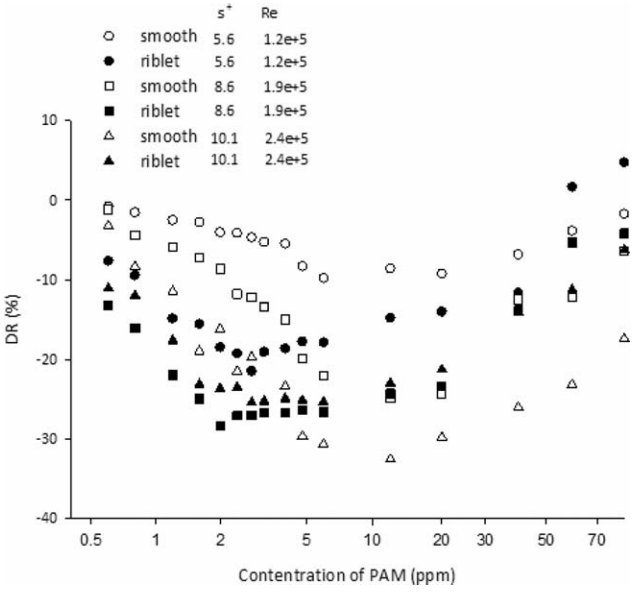

Figure 10. Drag reduction of tests in PAM solution.

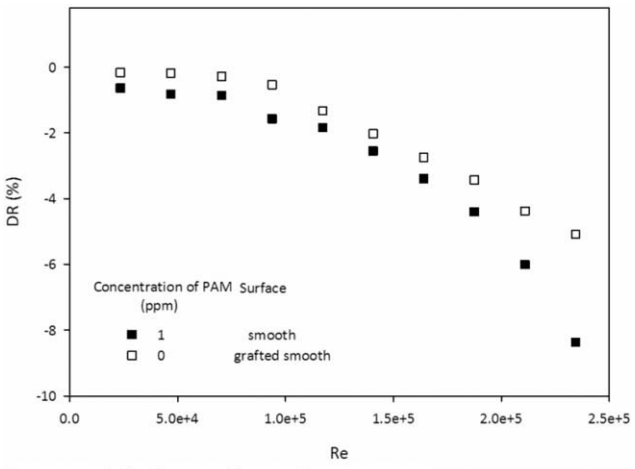

(a) Smooth surface

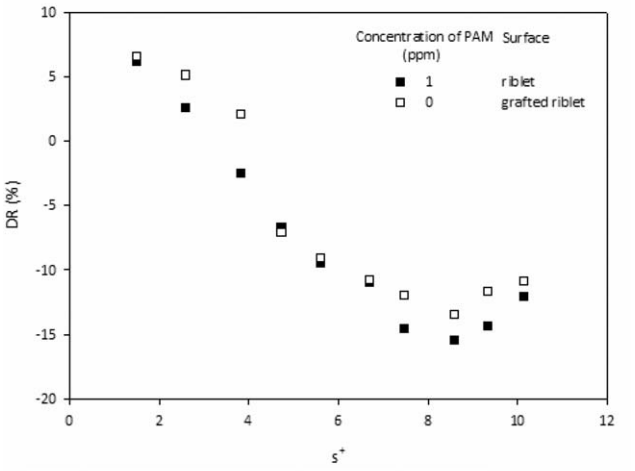

(b) Riblet surface

Figure 11. Drag reduction of grafted surface vs. PAM solution (1 ppm) for the smooth surface (a), and the riblet surface (b).

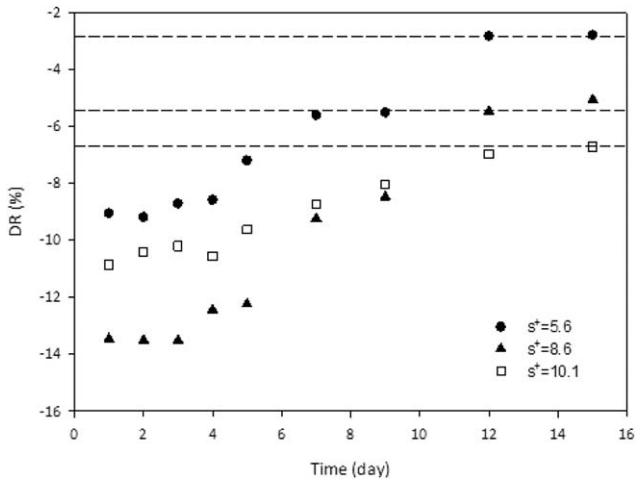

Figure 12. The *DR* of grafted riblet surface changes over time.

Figure 8. The drag reduction thin films are pasted onto both the outside and inside walls of the hollow barrel. This barrel is partly enclosed in the water-filled tank with a gap of approximately 5 mm from the bottom wall of the cup-shaped barrel to the water surface. Many holes are drilled into the bottom wall of the barrel to prevent air from squeezing inside the barrel after it is submerged into water. The used rotational viscometer is the Brookfield DV-III+ with a resolution of 0.01 Nm. The water bath is a cubic tank with a side length of 2 mm, and approximately 6000 L of water is used in the test. The water temperature of the tank is controlled at $20 \pm 1°C$, which is measured by a thermometer. The motor speed is adjusted and controlled by the computer, and the torque of the rotor is recorded to conduct drag reduction tests after rotating for 1 min to maintain stability. The smooth surface measurement is taken as the reference surface in order to calculate the drag reduction rate. The drag reduction rate *DR* can be represented by the difference between the test surfaces and the reference surfaces of the rotor torque as:

$$\%\mathrm{DR} = \frac{T_p - T_s}{T_s} \times 100\% \quad (2)$$

where T_s is the torque of the test rotor for a smooth surface and T_p is the torque used to test other drag reduction surfaces.

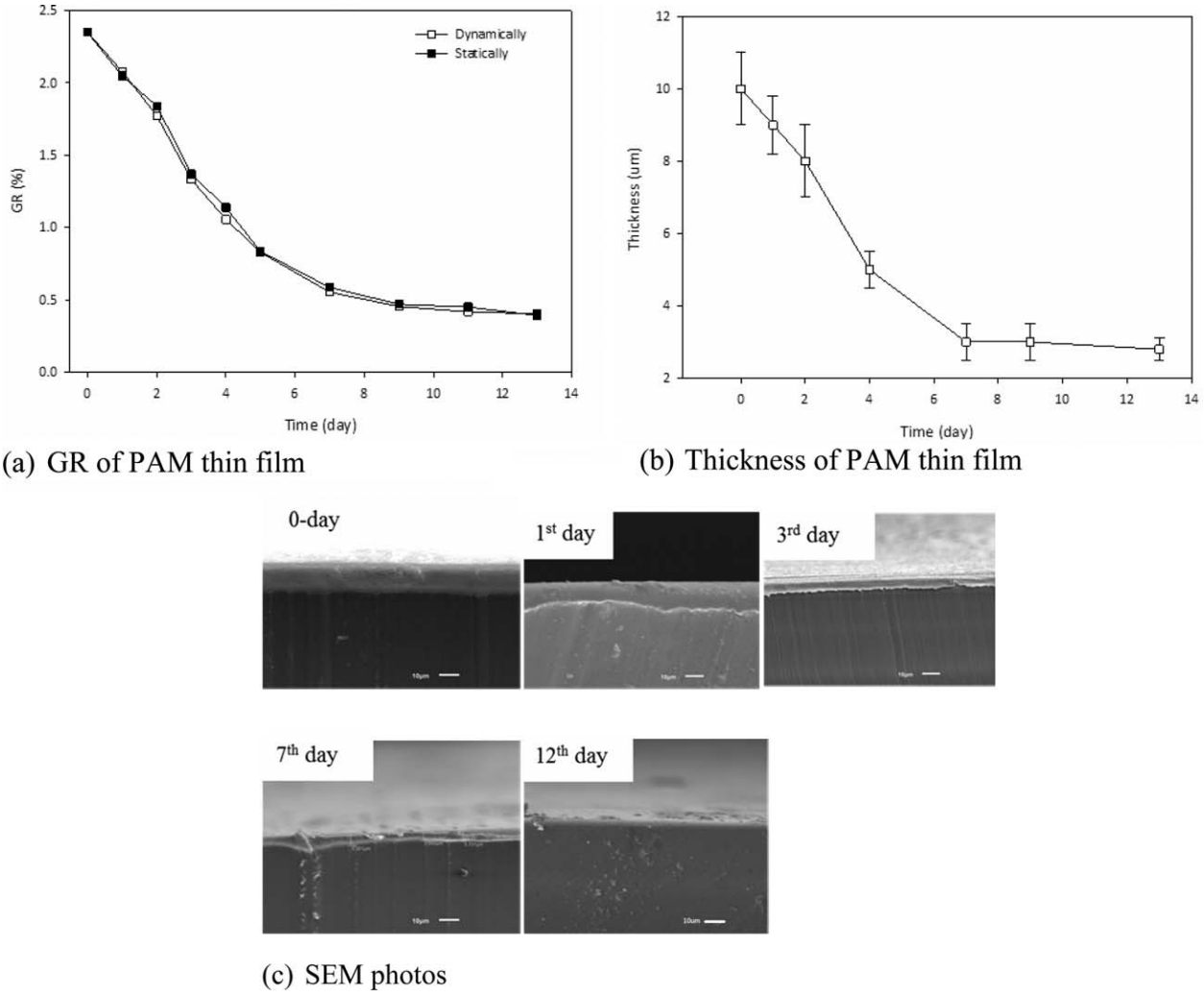

Figure 13. The variation of PAM thin film for the GR of grafted riblet surfaces (a), thickness (b), and SEM photos (c).

All of the surfaces—including the grafted smooth surface, the riblet surface, and the grafted riblet surface—are tested in order. The results of drag reduction are shown in Figure 9. We can see that as the test rotator rotates at a low velocity of about 10–30 cm s^{-1}, the riblet surface and the grafted riblet surface experience an increase in surface drag. Surface drag reduction can be achieved when the rotating velocity is at 40–100 cm s^{-1}. The drag reduction of the grafted riblet surface reaches a maximum at approximately 14.5% when the rotating velocity is approximately 80 cm s^{-1}. Under these conditions, the *DR* of the grafted riblet surface is larger than the sum of the riblet surface and the grafted smooth surface.

In order to verify whether the grafted drag reduction agent has the same mechanism as the drag reduction agent solution, drag reduction tests are carried out for a smooth surface and a riblet surface by varying the concentration of PAM in water. The solution concentration of PAM is adjusted by continuously adding PAM into the water tank during testing. The test results of the drag reduction are shown in Figure 10. No matter whether the surface riblets or the smooth surface, the value of *DR* initially increases and reaches a maximum of approximately 30% as the concentration of PAM increases. Later, the *DR* declines along with a continuous increase of PAM. By comparing the drag reduction of the PAM-grafted surface (Figure 9) with that of the test surface immersed in PAM solution, we can see that the grafted PAM is similar to the PAM solution in terms of the mechanism of drag reduction. Moreover, the *DR* of the grafted PAM approximately matches that of a 1 mg L^{-1} (ppm) concentration PAM solution, regardless of whether the surface used was smooth or riblet, as shown in Figure 11. The drag reduction of the riblet surface tested in pure water is in agreement with the traditional drag reduction of microgroove riblets, which also indicates that all of these tests are reliable.

Synthetic Surface Durability of Drag Reduction

To test the durability of the synthetic drag reduction surface, the grafted riblet surface is used as a test surface to conduct continuous tests in water for 15 days. The test rotor is immersed in water throughout the test and is rotated for 3 h to test drag reduction every day. Figure 12 shows the *DR* variation of the grafted riblet surface with the immersion time. The drag reduction performance of the test surfaces remains stable for the initial 3 days. The *DR* of the grafted riblet surface gradually declines to the level of the riblet surface after 12 days, which indicates that the grafted PAM dissolves out of the test surface, causing the synthetic drag reduction to disappear. Therefore, we surmise that the synthetic drag reduction performance may be maintained for approximately 12 days, which is much longer than that by simply painting PAM on to the surface of the test material. Grafted PAM is bonded to the substrate surface through chemical bonding. This grafted PAM results in a tangled agglomeration, which is shaped as a thin film on the surface. The PAM in the thin film commonly consists of main chains grafted on to the surface, while the branched chains are grafted on to the main chains. When the PAM thin film is immersed in fluid, the grafted main chains and branched chains can be slowly dissolved from the surface to act as drag reduction agents.

The variations of *GR* and the thickness of the PAM thin film over the period of immersion are shown in Figure 13. We can see that *GR* and the thickness of the PAM thin film initially decline and then gradually come to a constant state as the days of immersion increase, which does not change greatly with fluid flow. This indicates that the fluid flow has little impact on the *GR* or the thickness of the PAM thin film.

CONCLUSIONS

Polymer additives and microgroove riblets have been widely applied as conventional drag reduction approaches, although each approach has an inherent weakness. In this paper, UV-induced polymerization was investigated and synthetic drag reduction was achieved by grafting a PAM thin film onto the riblet surface of PVC. Infrared spectrum measurement was conducted to illustrate the grafting mechanism. Various tests were conducted to clarify the efficiency of UV-induced synthetic drag reduction. The following conclusions can be drawn:

1. Using UV grafting, the drag reduction agent PAM was grafted on to PVC substrates successfully. Within the scope of the tests, the maximum drag reduction rate of the synthetic drag reduction surface reached approximately 14%, which is higher than the traditionally used microgroove riblet.
2. The durability of UV-induced synthetic drag reduction was experimentally validated. The synthetic drag reduction of UV-induced polymerization can last well for 3 days and then declines gradually and finally disappears at approximately 12 days.

ACKNOWLEDGMENTS

This work was supported by National Natural Science Foundation of China (51175020) and National Natural Science Foundation of China Major Program (51290292).

REFERENCES

1. Elbing, B. R.; Winkel, E. S.; Lay, K. A.; Ceccio, S. L.; Dowling, D. R.; Perlin, M. *J. Fluid Mech.* **2008**, *612*, 201.
2. Chen, H.; Zhang, X.; Zhang, D.; Pan, J.; Hagiwara, I. *J. Appl. Polym. Sci.* **2013**, *130*, 2383.
3. Dean, B.; Bhushan, B. *Philos. Trans. Roy. Soc. A: Math. Phys. Eng. Sci.* **2010**, *368*, 4775.
4. Zhang, D.-Y.; Luo, Y.-H.; Li, X.; Chen, H.-W. *J. Hydrodyn. Ser. B* **2011**, *23*, 204.
5. Walsh, M. J. *AIAA J.* **1983**, *21*, 485.
6. Bechert, D.; Bruse, M.; Hage, W.; Van der Hoeven, J. T.; Hoppe, G. *J. Fluid Mech.* **1997**, *338*, 59.
7. Han, X.; Zhang, D.; Li, X.; Li, Y. *Chin. Sci. Bull.* **2008**, *53*, 1587.
8. Frings, B. *Rheol. Acta* **1988**, *27*, 92.
9. Anderson, G. W.; Rohr, J. J.; Stanley, S. D. *J. Fluids Eng.* **1993**, *115*, 213.
10. Mizunuma, H.; Yokouchi, Y.; Ueda, K. *J. Fluids Eng.* **1999**, *121*, 533.

11. Christodoulou, C.; Liu, K.; Joseph, D. *Phys. Fluids A: Fluid Dyn.* **1991**, *3*, 995.
12. Koury, E.; Virk, P. *Appl. Sci. Res.* **1995**, *54*, 323.
13. Choi, K.; Gadd, G.; Pearcey, H.; Savill, A.; Svensson, S. *Appl. Sci. Res.* **1989**, *46*, 209.
14. Zhang, D.; Li, Y.; Han, X.; Li, X.; Chen, H. *Chin. Sci. Bull.* **2011**, *56*, 938.
15. Deng, J.; Wang, L.; Liu, L.; Yang, W. *Prog. Polym. Sci.* **2009**, *34*, 156.
16. Cahalan, P. T.; Verhoeven, M. Google Patents, **1993**.
17. Yang, W.; Rånby, B. *J. Appl. Polym. Sci.* **1996**, *62*, 545.
18. Yang, W.; Rånby, B. *Macromolecules* **1996**, *29*, 3308.
19. Yang, W.; Rånby, B. *J. Appl. Polym. Sci.* **1996**, *62*, 533.
20. He, D.; Susanto, H.; Ulbricht, M. *Prog. Polym. Sci.* **2009**, *34*, 62.
21. Borcherding, H.; Hicke, H. G.; Jorcke, D.; Ulbricht, M. *Ann. NY Acad. Sci.* **2003**, *984*, 470.